DOI: 10.1002/cphc.200700840

Unique Reactivity of Confined Metal Atoms on a Silicon Substrate

Yun-Xi Yao,[a] Xin Liu,[a, b] Qiang Fu,*[a] Wei-Xue Li,*[a, b] Da-Li Tan,[a] and Xin-He Bao*[a]

Metal nanoclusters bridging the single atom and the bulk solid present many novel and size-dependent catalytic properties, which are otherwise absent from the bulk material. Extensive efforts have been made to understand the unusual reactivity of metal clusters of a few nanometers due to size effects.[1,2] For example, it is well-documented that the coupling of adsorbate orbitals to localized transition metal (TM) d bands is crucial and that it is mainly variation in the d-valence bands of various TMs that differentiates surface reactivity. Though sp electrons are also important for the overall bonding between TMs and molecules, they only play a small role in the differences in reactivity due to their free electron nature, which is similar for all TMs.[3] However, when metal clusters are composed of a few atoms, where orbital hybridization between the spatially confined atoms is greatly suppressed, the sp electrons become correspondingly discrete and localized. This localization is enhanced if the small metal ensembles are deposited on semiconducting or insulating substrates, where the sp electrons are further confined by the substrates due to the presence of the band gap. The change in the behaviour of the sp electrons of confined metal atoms on semiconducting or insulating substrates may have significant effects on the surface activity and selectivity, which could result in novel catalytic properties.[4,5]

To shed light on the electron confinement effect, in particular the sp electron confinement in supported metal atoms, and its effect on the surface reactivity, we report a comparative reactivity study of a bulk Ag(111) surface and an Ag monolayer film on an Si(111) surface by means of scanning tunneling microscopy (STM), ultraviolet and X-ray photoelectron spectroscopy (UPS and XPS), photoemission electron microscopy (PEEM), and density functional theory (DFT) calculations. An Si(111) surface is an ideal template for the growth of various quantum-confined metal nanostructures, for example, 2D quantum-well films and 0D quantum dots.[5,6] Particularly, Ag deposited on Si(111) can form a stable periodic array of Ag atoms confined in a 2D Ag monolayer film on Si(111) with ($\sqrt{3}\times\sqrt{3}$) symmetry (noted as $\sqrt{3}\times\sqrt{3}$-Ag–Si here), which has been subjected to extensive surface science studies as a classic metal/Si surface.[7–11] The simplest halogen methane, CCl_4, is chosen as the probe molecule to study the surface chemistry of the Ag surfaces due to its high reactivity towards Ag.[12–14] Our study shows that these two surfaces present distinct reactivities towards CCl_4 dissociation. Specifically, it is found that the confinement of the 5sp electrons of Ag [which is delocalized in the bulk Ag(111) surface] in the $\sqrt{3}\times\sqrt{3}$-Ag–Si surface is decisive in the different reactivities.

The $\sqrt{3}\times\sqrt{3}$-Ag–Si surface reported herein has a well-defined surface structure and morphology. This structure (the so-called inequivalent-triangle structure model[15]) contains an upper Ag monolayer, a second layer of Si trimers, and unreconstructed bulk Si substrate underneath.[7,8] The surface Ag atoms form two kinds of inequivalent Ag triangles: the Ag–Ag distance in the smaller triangles is 3.0 Å, and in the larger triangles is 3.9 Å. This is in contrast to 2.89 Å for Ag(111), as shown in Figure 1a, based on DFT calculations. The surface has a honeycomb structure[8,16] as seen in Figure 1b from a high-magnification STM image acquired at room temperature (RT). Here the bright protrusions lie at the centers of the Ag triangles (see inset in Figure 1b). From the UP spectra (Figure 1c), an energy gap of about 0.3 eV can be identified near the Fermi level (E_F) for the $\sqrt{3}\times\sqrt{3}$-Ag–Si surface.[17] The small gap indicates that the delocalized 5sp electrons observed on the metallic Ag(111) surface disappear in the energy range near E_F for the Ag monolayer grown on Si(111). Compared to Ag(111), the Ag 4d band of the $\sqrt{3}\times\sqrt{3}$-Ag–Si surface becomes sharp and narrow, because the topmost Ag atoms are well-separated. Furthermore, the weighted center of the Ag 4d band shifts downwards, which is confirmed by the DFT-calculated gap of 0.41 eV. XPS measurements (Figure 1d) show that there is a positive shift of 0.6 eV of the Ag 3d binding energy for the $\sqrt{3}\times\sqrt{3}$-Ag–Si surface relative to the Ag(111) surface. The calculated core level shift, 0.93 eV, is in line with the experimental measurement. These results show that the confined Ag atoms on the Si(111) substrate present significant differences in their electronic and structural properties in comparison to the bulk Ag surface.

The reactivity of these two surfaces is studied by exposing them to CCl_4. Figure 2a shows the UP spectra recorded from the Ag(111) surface exposed to 6 L of CCl_4 at 120 K and subsequently annealed at the temperatures indicated. At 120 K, there are four peaks 10.3, 7.2, 6.3, and 5.5 eV below E_F, which are attributed to the four molecular orbitals of CCl_4 ($2t_2$, 1e, $3t_2$, and $1t_1$, respectively) and indicate the multilayer molecular adsorption of CCl_4.[14] Upon an increase in temperature, the intensities of the four peaks decrease gradually due to desorption

[a] Y.-X. Yao, Dr. X. Liu, Dr. Q. Fu, Prof. Dr. W.-X. Li, D.-L. Tan, Prof. Dr. X.-H. Bao
State Key Laboratory of Catalysis
Dalian Institute of Chemical Physics
The Chinese Academy of Sciences
Zhongshan Road 457, Dalian 116023 (China)
Fax: (+86) 411-84694447
E-mail: xhbao@dicp.ac.cn
qfu@dicp.ac.cn

[b] Dr. X. Liu, Prof. Dr. W.-X. Li
State Key Laboratory of Catalysis and
Center for Theoretical and Computational Chemistry
Dalian Institute of Chemical Physics
The Chinese Academy of Sciences
Zhongshan Road 457, Dalian 116023 (China)
E-mail: wxli@dicp.ac.cn

Supporting information for this article is available on the WWW under http://www.chemphyschem.org or from the author.

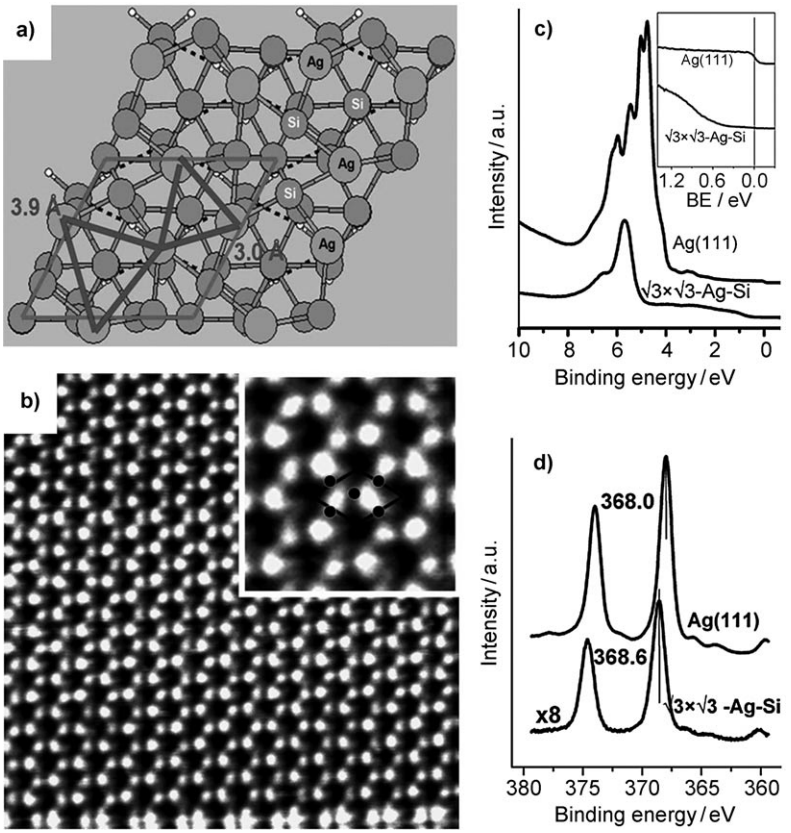

Figure 1. The atomic and electronic structures of the $\sqrt{3}\times\sqrt{3}$-Ag–Si surface. a) Structural model, where Ag and Si atoms are represented by large and small spheres, respectively. b) STM image of the $\sqrt{3}\times\sqrt{3}$-Ag–Si surface (15 nm×15 nm). c) UPS and d) Ag 3d XPS of the $\sqrt{3}\times\sqrt{3}$-Ag–Si and Ag(111) surfaces.

of the adsorbed CCl_4 molecules. When the surface is heated up to 135 K, new peaks at 8.7 and 3.5 eV due to dissociated $:CCl_2$ and Cl[14] occur. The spectral features of the $:CCl_2$ adsorbed on the surface remain unchanged up to 200 K, whereas further heating of the surface causes coupling of the adsorbed $:CCl_2$ to form C_2Cl_4, which desorbs completely at 224 K (Figure 2b). The peak at 3.5 eV arising from dissociated Cl increases with temperature and becomes dominant at RT. The inset (Figure 2b) suggests an increase in the surface work function by 0.4 eV during the annealing process.

The same procedures and conditions described above are also applied to the $\sqrt{3}\times\sqrt{3}$-Ag–Si surface, and the results are shown in Figure 2c. At 120 K, the same multilayer adsorption of CCl_4 occurs. However, upon annealing, the adsorbed CCl_4 molecules desorb from the surface intact, that is, without any dissociation, as also evidenced by temperature-programmed (TP)–UPS (not shown). This is further corroborated by the negligible variation in the surface work function (inset, Figure 2d). The apparent coverage of CCl_4 on the $\sqrt{3}\times\sqrt{3}$-Ag surface, which is calculated by the integration of the UPS area under 10.9 eV, shows roughly linear dependence on the annealing temperature in the range of 120–150 K. As shown in Figure 2d, complete desorption of CCl_4 occurs at 156 K and the UPS spectra recover the full features of a clean $\sqrt{3}\times\sqrt{3}$-Ag–Si surface.

The interaction of CCl_4 with the two Ag surfaces is studied by TP–XPS (see Figure 5 of the Supporting Information). Below 160 K, only molecular adsorption of CCl_4 is observed on the $\sqrt{3}\times\sqrt{3}$-Ag–Si surface, whereas significant dissociation occurs on the Ag(111) surface above 135 K, which is fully consistent with the UPS results.

The mechanism behind the different reactivities towards CCl_4 of both surfaces is studied by DFT calculations. For CCl_4 adsorption on the Ag(111) and $\sqrt{3}\times\sqrt{3}$-Ag–Si surfaces, many configurations are explored, and two kinds of geometries are identified: 1) one Cl atom points towards the surface, and the remaining three Cl atoms point towards the vacuum, 2) the reversal of configuration (1). The centers of mass of the adsorbed CCl_4 molecules are placed at top, bridge and hollow sites with respect to the substrates underneath. It turns out that CCl_4 binds weakly to both surfaces, independently of its orientation and adsorption site. The interaction between CCl_4 and Ag(111) is slightly stronger than that between CCl_4 and $\sqrt{3}\times\sqrt{3}$-Ag–Si, and the calculated adsorption energy for the favorable configurations are −0.17 and −0.10 eV (exothermic), respectively. The small adsorption energy on both surfaces agrees well with the low desorption temperatures observed experimentally. To study the reactivity of these two surfaces, the various dissociation paths and activation barriers for breaking the first C–Cl bond of CCl_4 are calculated by using the nudged elastic band method. It is found that the activation barrier on Ag(111) is generally 0.60–0.70 eV lower than on $\sqrt{3}\times\sqrt{3}$-Ag–Si. To illustrate this point, the calculated potential energy surfaces for configuration (1) are shown in Figure 3a. On the right-hand side the initial configurations of the adsorbed CCl_4 on the two surfaces are shown. The activation barriers of 0.194 eV for Ag(111) and 0.945 eV for $\sqrt{3}\times\sqrt{3}$-Ag–Si are shown. Both the activation energy for C–Cl bond breaking and the CCl_4 adsorption energy on Ag(111) are modest and comparable, which show that desorption and dissociation of the adsorbed CCl_4 molecules are facile and competitive processes on Ag(111)—exactly as found experimentally. In contrast to this, the activation energy for C–Cl bond breaking on $\sqrt{3}\times\sqrt{3}$-Ag–Si is significantly larger than the CCl_4 adsorption energy, which indicates that CCl_4 molecular desorption is the dominant process taking place on $\sqrt{3}\times\sqrt{3}$-Ag–Si at elevated temperatures.

To determine the origin of the dramatically different reactivities of these two surfaces, we perform an electronic structure analysis. The projected density of states (PDOS) of the products

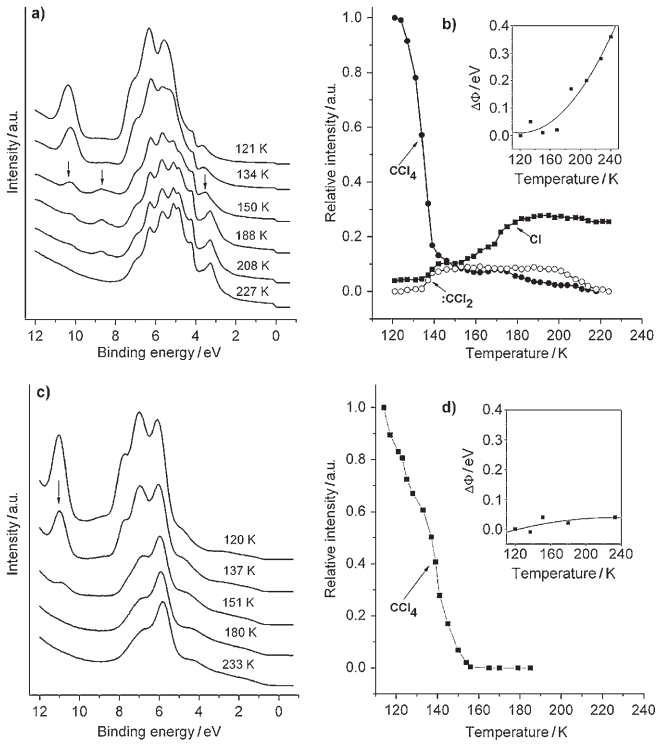

Figure 2. a) UPS (He I) of 6 L CCl_4 pre-covered Ag(111) at 120 K and annealed to the temperatures indicated. b) Normalized integrated areas of the peaks at about 10.3, 8.7, and 3.5 eV on Ag(111) at different annealing temperatures. The inset shows the work function change ($\Delta\Phi$) during annealing. c) UPS (He I) of 6 L CCl_4 pre-covered $\sqrt{3}\times\sqrt{3}$-Ag–Si surface at 120 K and annealed to the temperatures indicated. d) Normalized integrated areas of the peak at about 10.9 eV on the $\sqrt{3}\times\sqrt{3}$-Ag–Si surface at different annealing temperatures. The inset shows the work function change ($\Delta\Phi$) during annealing.

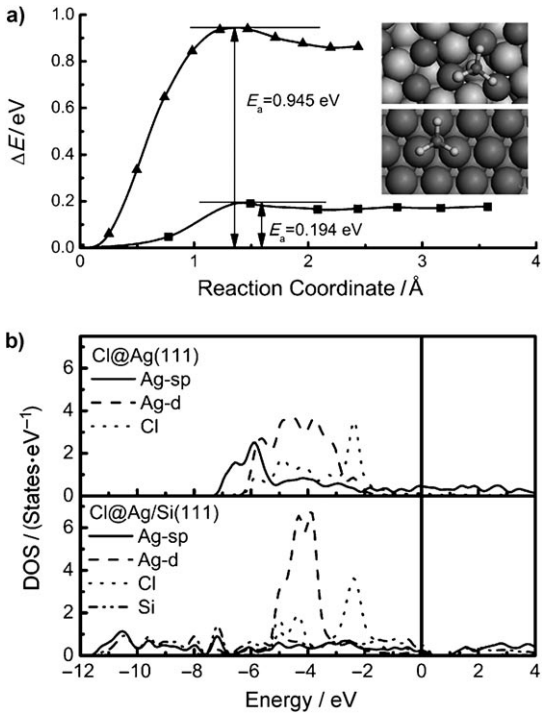

Figure 3. a) Calculated potential energy surfaces for CCl_4 dissociation on the Ag(111) (■) and $\sqrt{3}\times\sqrt{3}$-Ag–Si (▲) surfaces. The structures for the initial states are shown schematically in the inset, where Ag and Si atoms are represented by large grey and white spheres, respectively, and small grey and white spheres represent C and Cl atoms, respectively. b) Calculated projected density of states for dissociated Cl atom adsorbed on Ag(111) (upper) and $\sqrt{3}\times\sqrt{3}$-Ag–Si (lower). Ag 5 sp, Ag 4d, Cl, and Si PDOS, are represented by (——), (- - - -), (•••••) and (–•–•) respectively.

(the dissociated Cl atom adsorbs at the center of three surface Ag atoms of the two surfaces) are shown in Figure 3 b. For Ag(111) [the upper graph in Figure 3 b], the Cl 3p orbital hybridizes not only with the Ag 4d band, but also with the Ag 5sp band, which contributes a significant peak around −5.90 eV. These two interactions result in a strong chemical bond between the dissociated Cl atoms and Ag(111). The calculated dissociative adsorption energy of the Cl atom (with respect to the Cl_2 molecules in the gas phase) is −1.48 eV. The PDOS for Cl adsorbed on the $\sqrt{3}\times\sqrt{3}$-Ag–Si surface are shown in Figure 3 b (lower graph). As mentioned earlier, there is a downshift of the weighted center of the Ag 4d band (0.41 eV) from the clean Ag(111) to the clean $\sqrt{3}\times\sqrt{3}$-Ag–Si surfaces, which may weaken the interaction between Cl and Ag.[3,18] Furthermore, the hybridization between the Cl 3p orbital and the Ag 5sp band, as found in Ag(111) around −5.90 eV, is totally absent for the $\sqrt{3}\times\sqrt{3}$-Ag–Si surface. Instead, a broad resonance at an energy window of [−12 eV, 0 eV] (relative to E_F) appears due to the hybridization between the Ag 5sp band and the Si 3sp orbital, and the interaction between Cl and the $\sqrt{3}\times\sqrt{3}$-Ag–Si surface is further weakened. Together, these two factors result in a significant decrease in the overall bonding between Cl and $\sqrt{3}\times\sqrt{3}$-Ag–Si, and the calculated adsorption energy of the Cl atom is −0.93 eV. Thus, CCl_4 dissociation becomes thermodynamically less driven and the C–Cl bond breaking becomes highly demanding.

This analysis highlights the importance of the Ag 5sp electrons to reactivity. Since the Ag 4d bands of both surfaces are fully occupied and localized, corresponding charge transfer to the approaching molecules is similar for both. On the metallic Ag(111) surface, delocalized Ag 5sp electrons can easily be transferred to the approaching molecules, which facilitates C–Cl bond-breaking and Ag–Cl bond-making. However, for the $\sqrt{3}\times\sqrt{3}$-Ag–Si surface, the Ag 5sp electrons of the confined Ag atoms on silicon is localized at the Ag–Si interface and the Ag 5sp orbitals cannot hybridize with the approaching molecules. The amount of charge transfer between the approaching molecules and the $\sqrt{3}\times\sqrt{3}$-Ag–Si surface decreases correspondingly, and the processes of bond-breaking and -making become quite demanding. It is therefore the confinement of the Ag 5sp electrons of the Ag atoms deposited on the silicon substrates that prevents C–Cl bond-breaking on the $\sqrt{3}\times\sqrt{3}$-Ag–Si surface.

Having established the origin of the different reactivities of the two surfaces, the reaction dynamics was further studied by in situ PEEM at RT on specially prepared silver particles possessing various facets and defects, instead of the perfect Ag(111) surface used up to now. Starting from the $\sqrt{3}\times\sqrt{3}$-Ag–Si surface, these particles are prepared by depositing additional

Ag atoms at RT. These agglomerate into Ag crystallites on the surface, which co-exist with the bare $\sqrt{3}\times\sqrt{3}$-Ag–Si surface[19], as schematically shown in Figure 4a and imaged clearly by PEEM (Figure 4b). The bright regions (marked as A) are from the bulk Ag islands with a size of a few μm and the dark regions are the $\sqrt{3}\times\sqrt{3}$-Ag–Si surface (marked as B). After exposure to 24 L CCl_4, the image contrast at the two regions was reversed completely (Figure 4c). In situ imaging of the surface reaction shows a gradual change in the grey intensity from bright to totally dark on the Ag islands during the CCl_4 exposure with little change on the $\sqrt{3}\times\sqrt{3}$-Ag–Si surface. The large decrease in the grey intensity of the Ag islands due to the significant increase of the local work function from the dissociated Cl atoms unambiguously shows surface reactions taking place on the bulk Ag surface but not on the $\sqrt{3}\times\sqrt{3}$-Ag–Si region. This is fully consistent with the PES results on the perfect Ag(111) and $\sqrt{3}\times\sqrt{3}$-Ag–Si surfaces (see Figure 4d and from the Supporting Information, Figure 6). Since the agglomerated silver islands are large enough to maintain metallic features, the high reactivity of the silver islands in comparison to the $\sqrt{3}\times\sqrt{3}$-Ag–Si surface observed by in situ PEEM further shows the essential role of metallicity and, therefore, the importance of the free sp electrons of Ag in the surface reactivity, independent of island size, facet orientations and defects.

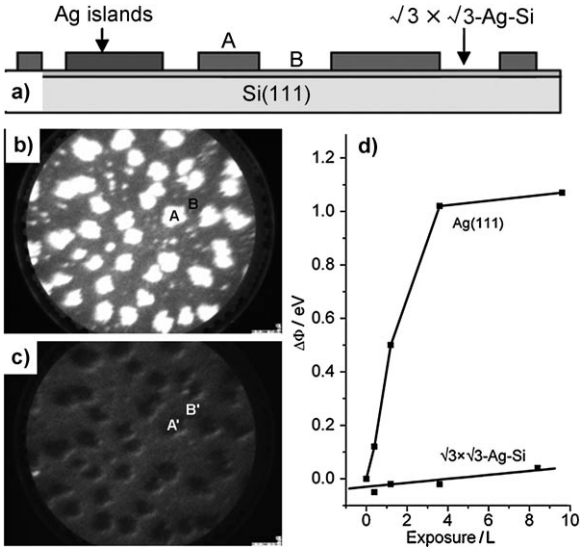

Figure 4. a) Schematic representation of the $\sqrt{3}\times\sqrt{3}$-Ag–Si-surface-supported Ag islands. b) PEEM image of the Ag islands/$\sqrt{3}\times\sqrt{3}$-Ag–Si sample before CCl_4 exposure. The field of view is 27 μm. c) PEEM image shows the same area as in (b) but after 24 L (5.2×10^{-9} mbar × 6000 s) CCl_4 exposure. d) The work function change ($\Delta\Phi$) of the Ag(111) and $\sqrt{3}\times\sqrt{3}$-Ag–Si surfaces when exposed to different amounts of CCl_4 at RT, measured from PES results (see Figure 6 in the Supporting Information).

In conclusion, the distinct reactivity of the Ag monolayer deposited on the Si substrate with respect to the bulk Ag surface, was observed. The origin of the unusual reactivity of the Ag monolayer on Si(111) is identified to be the confinement of valence electrons, particularly the Ag 5sp electrons in the Si(111)-supported Ag adatoms. In the past, it was found that the confinement of sp electrons in 2D films due to formation of quantum well states is capable of tuning the surface reactivity of sp metals, such as Pb[5] and Mg[20]. The present work shows that even when a transition metal has d electrons, its sp electrons can be modified and/or confined by careful fabrication of the metal layers on semiconducting or insulating substrates, to influence the surface reactivity dramatically.

Experimental Section

All experiments were performed in an Omicron multiple-chamber ultrahigh vacuum (UHV) system installed with a hemisphere analyzer (Omicron EA125 5-channeltron), a photoemission electron microscope (Focus IS–PEEM), and a scanning tunneling microscope (Omicron VT AFM), which has been described elsewhere.[6] The XPS spectra were acquired with Mg Kα (1253.6 eV) radiation. Binding energies were calibrated using Ag $3d_{5/2}$ at 368 eV. All UP spectra were recorded with He I (21.2 eV) radiation in the normal emission direction. PEEM images were recorded using a 100 W mercury short-arc lamp with the photon energy of the main UP line at about 4.9 eV as a radiation source. All STM images were recorded in constant current mode using a W-tip at RT.

A single crystal of Ag(111) was cleaned by repeated Ar^+ sputtering (1000 eV, 20 μA, 1200 s) and annealing (873 K, 600 s) until no contaminations were detected. Clean Si(111)-7×7 reconstructed surfaces were obtained by repeated direct current heating of single crystal Si(111) slices (*n*-doped, 0.53–0.56 Ω cm, approximately 3×10×0.5 mm^3 in dimension) to 1200 °C. The $\sqrt{3}\times\sqrt{3}$-Ag–Si surfaces were prepared by evaporating 1 monolayer (ML) Ag onto the Si-(111)-7×7 (the number density of Si atoms on the Si(111) surface) at 550 K or depositing 1 ML Ag on Si(111)-7×7 at RT and subsequently annealing to 600 K. HPLC-grade CCl_4 was used as received. Before each dosing experiment, the CCl_4 was purified by several freeze-pump-thaw cycles. Sample dosing was performed by backfilling the vacuum chamber via a leak valve. Exposures are given in Langmuir units (1 L = 1×10^{-6} Torr s) uncorrected for ion gauge sensitivity.

Our calculations use the ultrasoft pseudopotential plane wave codes[18] with a kinetic cutoff of 25 Ry, and the generalized-gradient Perdew–Wang91 functional.[22] Optimized lattice constants (4.14 Å for Ag and 5.47 Å for Si) were used throughout the calculations. Four layers of slab separated by at least 15 Å vacuum were used to simulate the surfaces, and adsorbates were placed at one side of the slab with dipole correction. For the $\sqrt{3}\times\sqrt{3}$-Ag–Si surface, the bottom of silicon substrate was saturated by hydrogen atoms. The SBZ sampling was carried out with a (4×4×1) grid in the Monkhorst–Pack scheme[21] for Ag(111)-(2×2) and primitive $\sqrt{3}\times\sqrt{3}$-Ag–Si surface. The adsorbates and top two substrate layers were fully relaxed until the residual forces less than 0.02 eV $Å^{-1}$. The transition states were calculated using nudged elastic band method with care being taken that the pathways become continuous.

Acknowledgements

We acknowledge financial support from NSFC (20503030, 20573107, 20603037, 20733008), MOST (2007CB815205) and CAS "Bairen Project".

Keywords: chemisorption · confinement effects · density functional calculations · photoemission electron microscopy · size effects

[1] H.-J. Freund, *Surf. Sci.* **2002**, *500*, 271–299.
[2] M. S. Chen, D. W. Goodman, *Acc. Chem. Res.* **2006**, *39*, 739–746.
[3] B. Hammer, J. K. Norskov, *Adv. Catal.* **2000**, *45*, 71–129.
[4] G. Pacchioni, L. Giordano, M. Baistrocchi, *Phys. Rev. Lett.* **2005**, *94*, 226104.
[5] X. C. Ma, P. Jiang, Y. Qi, J. F. Jia, Y. Yang, W. H. Duan, W. X. Li, X. H. Bao, S. B. Zhang, Q. K. Xue, *Proc. Natl. Acad. Sci. USA* **2007**, *104*, 9204–9208.
[6] Z. Zhang, Q. Fu, H. Zhang, Y. Li, Y. X. Yao, D. L. Tan, X. H. Bao, *J. Phys. Chem. C* **2007**, *111*, 13524–13530.
[7] M. Katayama, R. S. Williams, M. Kato, E. Nomura, M. Aono, *Phys. Rev. Lett.* **1991**, *66*, 2762–2765.
[8] T. Takahashi, S. Nakatani, N. Okamoto, T. Ishikawa, S. Kikuta, *Surf. Sci.* **1991**, *242*, 54–58.
[9] S. Hasegawa, X. Tong, S. Takeda, N. Sato, T. Nagao, *Prog. Surf. Sci.* **1999**, *60*, 89–257.
[10] L. Chen, H. J. Xiang, B. Li, A. Zhao, X. Xiao, J. Yang, J. G. Hou, Q. Zhu, *Phys. Rev. B* **2004**, *70*, 245431.
[11] M. Ono, Y. Nishigata, T. Nishio, T. Eguchi, Y. Hasegawa, *Phys. Rev. Lett.* **2006**, *96*, 016801.
[12] St.-J. Dixon-Warren, E. T. Jensen, J. C. Polanyi, *Phys. Rev. Lett.* **1991**, *67*, 2395–2398.
[13] W. Huang, J. M. White, *J. Am. Chem. Soc.* **2004**, *126*, 14527–14532.
[14] N. Bovet, D. I. Sayago, F. Allegretti, E. A. Kröger, M. J. Knight, J. Barrett, D. P. Woodruff, R. G. Jones, *Surf. Sci.* **2006**, *600*, 241–248.
[15] H. Aizawa, M. Tsukada, N. Sato, S. Hasegawa, *Surf. Sci.* **1999**, *429*, L509–L514.
[16] T. Takahashi, S. Nakatani, N. Okamoto, T. Ishikawa, S. Kikuta, *Jpn. J. Appl. Phys. Part 2* **1988**, *27*, L753–L755.
[17] J. Viernow, M. Henzler, W. L. O'Brien, F. K. Men, F. M. Leibsle, D. Y. Petrovykh, J. L. Lin, F. J. Himpsel, *Phys. Rev. B* **1998**, *57*, 2321–2326.
[18] B. Hammer, L. B. Hansen, J. K. Norskov, *Phys. Rev. B* **1999**, *59*, 7413–7421.
[19] V. A. Gasparov and M. Riehl-Chudoba, http://arxiv.org/abs/0708.4148v1.
[20] L. Aballe, A. Barinov, A. Locatelli, S. Heun, M. Kiskinova, *Phys. Rev. Lett.* **2004**, *93*, 196103.
[21] J. P. Perdew, J. A. Chevary, S. H. Vosko, K. A. Jackson, M. R. Pederson, D. J. Singh, C. Fiolhais, *Phys. Rev. B* **1992**, *46*, 6671–6687.
[22] H. J. Monkhorst, J. D. Pack, *Phys. Rev. B* **1976**, *13*, 5188–5192.

Received: December 17, 2007
Published online on March 20, 2008

